



OPEN

A pore-occluding phenylalanine gate prevents ion slippage through plant ammonium transporters

Pascal Ganz, Robin Mink , Toyosi Ijato, Romano Porras-Murillo, Uwe Ludwig  & Benjamin Neuhäuser*

Throughout all kingdoms of life, highly conserved transport proteins mediate the passage of ammonium across membranes. These transporters share a high homology and a common pore structure. Whether NH_3 , NH_4^+ or $\text{NH}_3 + \text{H}^+$ is the molecularly transported substrate, still remains unclear for distinct proteins. High-resolution protein structures of several ammonium transporters suggested two conserved pore domains, an external NH_4^+ recruitment site and a pore-occluding twin phenylalanine gate, to take over a crucial role in substrate determination and selectivity. Here, we show that while the external recruitment site seems essential for AtAMT1;2 function, single mutants of the double phenylalanine gate were not reduced in their ammonium transport capacity. Despite an unchanged ammonium transport rate, a single mutant of the inner phenylalanine showed reduced N-isotope selection that was proposed to be associated with ammonium deprotonation during transport. Even though ammonium might pass the mutant AMT pore in the ionic form, the transporter still excluded potassium ions from being transported. Our results, highlight the importance of the twin phenylalanine gate in blocking uncontrolled ammonium ion flux.

Ammonium is one of the major inorganic nitrogen sources for plants. In *Arabidopsis thaliana*, other plants and organisms from all kingdoms of life, ammonium is transported across membranes by proteins of the AMT (AMmonium Transporter) / Rh (Rhesus protein)/Mep (Methylammonium permease) family.

The uptake of ammonium (here referring to the sum of NH_3 and NH_4^+) was comprehensively studied in model organisms, where it has been shown that ammonium can be taken up against its concentration gradient. This results in a significant accumulation of ammonium within cells^{1–4}. At acidic pH, the NH_4^+ ion is by orders of magnitude more abundant than NH_3 ($\text{pK}_a = 9.25$). The uptake of ammonium by plants is biphasic and is constituted of a high-affinity transport system component (HATS) and a low-affinity transport system component (LATS). AMT proteins build the plant ammonium HATS, while the molecular identity of the ammonium LATS remains elusive⁵. Plant AMTs further split into transport proteins conducting net ammonium ($\text{NH}_3 + \text{H}^+$) transport (AMT1s) and AMT2-like transporters, conducting NH_3 ^{6–10}.

Protein structures of AMT proteins from bacteria and archaea allow comparisons of the pore structures of different AMTs^{11–13}. It is striking that otherwise diverse AMTs like AtAMT1;2 and EcAmtB (*E. coli* Ammonium transporter B) share very high identity in their pore-lining residues^{7,9}. A close look at the pore structure of EcAmtB shows a conserved outer recruitment site for NH_4^+ with the amino acid residue Asp₁₆₀ serving as countercharge to stabilize the recruited NH_4^+ ^{14–17}. This aspartic acid residue was further proposed to hold an important function in stabilizing the AMT protein structure^{11,12,14,15,18}. A conserved serine^{11,16,19} and alanine¹⁷ appear to be involved in replacing the water in the hydration shell of NH_4^+ before it enters the AMT pore^{12,15,20}.

After the recruitment of NH_4^+ at the external vestibule, deprotonation to ammonia was proposed by studies on structural constraints and molecular dynamics simulation on the ammonium transport mechanism of the AMT/Rh/Mep proteins. Different sites of deprotonation were suggested^{14–16,18,20–28}. Directly adjacent to the NH_4^+ recruitment site, a pore-occluding double phenylalanine gate appears to block further transport of NH_4^+ into the pore. Some computational studies proposed that deprotonation of the substrate might occur during the translocation from the external vestibule to the inside of the pore, while passing the phenylalanine gate^{15,16,18,20,26}. Other studies suggested that the ammonium ion is guided into the channel lumen, crossing the phenylalanine gate before it is deprotonated at the position of a conserved twin-His structure^{14,21}. Mutational studies of the

Institute of Crop Science, Nutritional Crop Physiology, University of Hohenheim, Fruwirthstr. 20, 70593, Stuttgart, Germany. *email: benjamin.neuhaeuser@uni-hohenheim.de

two phenylalanines in EcAmtB highlighted their importance in the ammonium transport mechanism. Exchange of F₁₀₇ by alanine and leucine yielded a completely active transporter^{19,29}, but the second Phe was important for the transport function. Replacement of the second phenylalanine by leucine strongly reduced ammonium uptake, as well as methylammonium transport^{19,29}. Change of this inner phenylalanine to alanine inactivated the transporter. Most double mutants of the phenylalanines in EcAmtB e.g. the F₁₀₇A F₂₁₅A mutant were completely inactive in ammonium transport¹⁹. This inactive double phenylalanine to alanine mutant potentially mimics the configuration of an “open” transport pathway. Molecular dynamics simulations of ammonium transport by this mutant proposed that NH₄⁺ is stabilized by the protein backbone at the position of the phenylalanine gate. As a consequence, ammonium deprotonation during its transportation occurs beyond the Phe-gate¹⁹ possibly at the adjacent conserved twin-His structure. This implies that the phenylalanine gate might not directly be involved in substrate deprotonation.

Ammonium transport in mutants lacking both phenylalanines could partially be rescued by introducing another mutation, W₁₄₈L^{19,29}. This rescue was not due to charge stabilization in the external vestibule, as W₁₄₈ was computed to be only of minor importance for stabilizing the ammonium charge in the binding site¹⁴. Introduction of the W₁₄₈L mutation strongly increased methylammonium transport in AmtB. Mutations in the corresponding residue in an AMT1;1 from tomato reduced transport rates for NH₄⁺ and MeA⁶. In consequence, it was argued that the double phenylalanine gate is dispensable for transport by EcAmtB²⁹.

When addressing the function of the Phe-gate in the human RhCG transporter, already a mutation of one of the Phe residues resulted in a dramatic activity loss. Interestingly, the double mutant, which is non-functional in EcAmtB, was active in RhCG³⁰. The combined results point to a species-specific importance of the external vestibule and the Phe-gate in distinct ammonium transporters.

The Phe-gate function has not yet been investigated for the functionally unique AMT1 net ammonium transporters from plants. We hypothesized that the Phe-gate is dispensable for function. Here we analyzed the role of the Phe-gate and the conserved residues in the external vestibule in substrate recruitment, deprotonation and selectivity of AtAMT1;2.

Results

The function of the NH₄⁺ recruitment pocket residues is conserved between plant and bacterial transporters. Multiple studies highlighted three highly conserved amino acid residues to be essential in electrostatic stabilization of the charged substrate in the NH₄⁺ recruitment pocket^{11–13}. Based on a structural alignment and homology modeling, previous studies identified the respective residues in AtAMT1;2^{7,10}. Asp₂₁₁, Ala₂₁₃ as well as Ser₂₇₅ (Fig. 1) were proposed to either coordinate the substrate or stabilize the substrate charge within the external vestibule^{14–17}. We addressed the importance of these residues in AtAMT1;2 by changing them into glycine residues and tested functionality of the mutants in yeast. AtAMT1;2 or AtAMT2 rescued yeast growth of an ammonium transporter-deficient yeast strain ($\Delta\Delta\Delta mep$) with ammonium as sole nitrogen source^{8,31}. Asp₂₁₁ and Ser₂₇₅ have side chains possibly involved in direct hydrogen bonding with NH₄⁺. While Asp₂₁₁ is essential for transport activity, the S₂₇₅G mutant showed negligible residual activity (Figs 1; S1). Albeit, the A₂₁₃G mutation did not affect transporter activity.

The highly conserved pore-occluding Phe-gate is not essential for transport. The Phe-gate (F₁₄₇ and F₂₇₁) (Fig. 1) is highly conserved throughout the AMT/Rh/Mep protein family, as it is exhibited by plant AMTs from important model and crop plants like *Arabidopsis thaliana* (AtAMT), *Medicago truncatula* (MtAMT), *Lycopersicon esculentum* (LeAMT), *Oryza sativa* (OsAMT) and *Triticum aestivum* (TaAMT). The neighbouring amino acids residues are highly conserved as well, implying a conserved function in the pore region (Fig. S2). Phenylalanine mutants were analyzed by mutation and growth complementation in $\Delta\Delta\Delta mep$ yeast (Fig. 2).

Single alanine replacements of individual phenylalanines to alanine were tolerated, which in part is in contrast to the situation in EcAmtB, while the simultaneous exchange of both Phe-gate residues abolished ammonium transport (Figs 2; S3). A further amino acid residue, W₁₈₈, was included in the analysis by introducing a W₁₈₈A or W₁₈₈L mutation. Mutation of this residue was able to rescue a Phe double mutant in EcAmtB²⁹.

The transport activity of these mutants was then quantified in liquid culture using an ammonium uptake assay. Negligible residual flux of ammonia into the cells was observed in empty vector controls, while both single Phe mutants retained wildtype AtAMT1;2 transport capacity (Fig. 3). The double mutant did not show significant ammonium uptake, but some residual transport was conferred by the additional W₁₈₈L mutation. Thus, a single Phe is sufficient to maintain plant AMT1;2 ammonium transport function, while double mutants lacking both pore Phe residues were largely inactive.

Mutation of W₁₈₈ to Ala or Leu established profound MeA transport by the double mutant. In the AMT1;2 single and double Phe mutants, the ability to transport ammonium directly correlated with the capacity to import the toxic analog MeA, which then impaired yeast growth (Figs 4; S3). While the triple mutants F₁₄₇A F₂₇₁A W₁₈₈A/L failed to transport ammonium (Figs 2, 3), they transported MeA, in contrast to the F₁₄₇A F₂₇₁A double mutant (Fig. 4).

The combined results identify similarity to the situation in EcAmtB and suggest that loss of both Phe in AtAMT1;2 can be compensated by an additional mutation in W₁₈₈ for the substrate MeA but not for ammonium.

Mutation of Phe₂₇₁ may result in ion slippage through the AtAMT1;2 pore. In the proposed AMT transport mechanism with NH₄⁺ recruitment, deprotonation and finally conduction of NH₃ in the hydrophobic pore¹⁹, the fate of the proton remained controversial. The basic mechanism of deprotonations was, however, strongly supported by the identification of $\delta^{15}\text{N}$ shifts caused by ammonium uptake into yeast cells³². Discrimination against the heavier isotope was interpreted as a direct indication for deprotonation of the

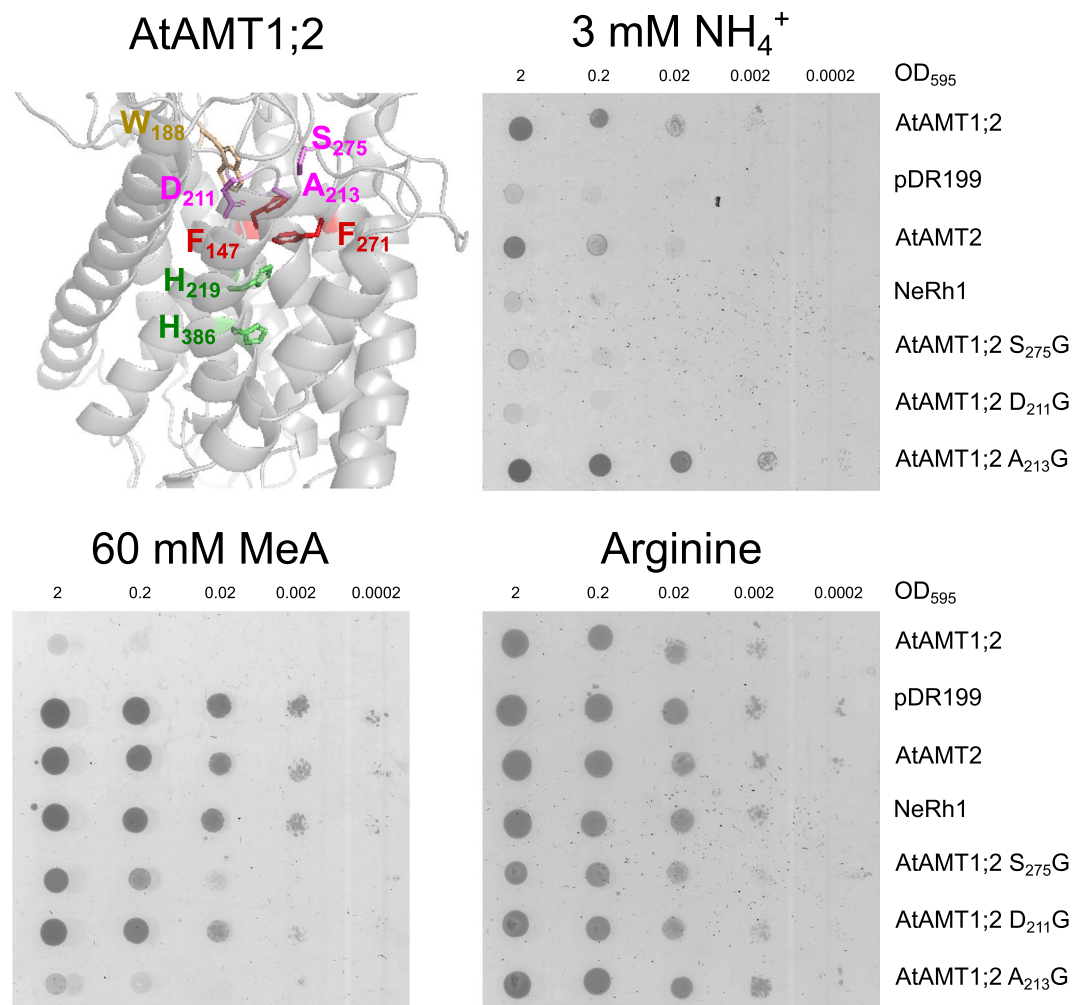


Figure 1. Functional assessment of recruitment pocket mutants by complementation of the $\Delta\Delta\Delta mep$ yeast. Homology model of AtAMT1;2 (top left) based on the ScMEP2 protein structure³⁷. The model shows the location and orientation of the amino acid residues investigated in this study (D₂₁₁, A₂₁₃, S₂₇₅ in the recruitment pocket, the Phe gate F₁₄₇ and F₂₇₁, W₁₈₈ and the twin His motif H₂₁₉ and H₃₈₆). $\Delta\Delta\Delta mep$ yeast was transformed with empty vector (pDR199) or pDR199 containing wildtype or mutant AtAMTs as well as NeRh1. The transformed yeast was spotted in 10-fold dilutions beginning with an OD₅₉₅ = 2 on media containing arginine (control = bottom right), ammonium (3 mM = top right) as sole nitrogen source or Arginine with 60 mM MeA (bottom left). Yeast growth on ammonium indicates ammonium transport, while no growth on toxic MeA indicates MeA uptake. Three independent repetitions have been performed, the figure shows one representative experiment.

substrate in AMT proteins³². The AtAMT1;2 wildtype, as well as the F₁₄₇A single mutant, showed strong isotope discrimination. Interestingly, all variants bearing the F₂₇₁A mutation showed a decreased discrimination of the heavier isotope (Fig. 5), potentially indicating a reduced NH₄⁺ deprotonation and an increase in ion slippage through the mutant AtAMT1;2 pore.

Reduced isotope discrimination is not accompanied by a compromised selectivity against K⁺. Deprotonation of the substrate elegantly explains the high ammonium selectivity of AMT proteins against the similarly-sized K⁺. Therefore, the possibility of K⁺ conduction by the mutants harboring the F₂₇₁A mutation was considered in this study. We hypothesized that if the F₂₇₁A mutant allows NH₄⁺ ion slippage through the central pore, it may as well allow K⁺ transport. Potassium transport capacity was tested in the W Δ 3 yeast strain which lacks two endogenous potassium transporters. This yeast was transformed with all active transporter variants and grown on media containing low mM K⁺ concentrations. Improved growth of the yeast on this medium would indicate facilitated K⁺ transport. None of the transformed transporter variants was able to promote yeast growth (Figs 6, S4). By contrast all constructs slightly impaired growth on high K⁺. This result probably indicates unspecific negative effects by each construct, as the non-functional mutant had the largest impairment relative to the empty plasmid control.

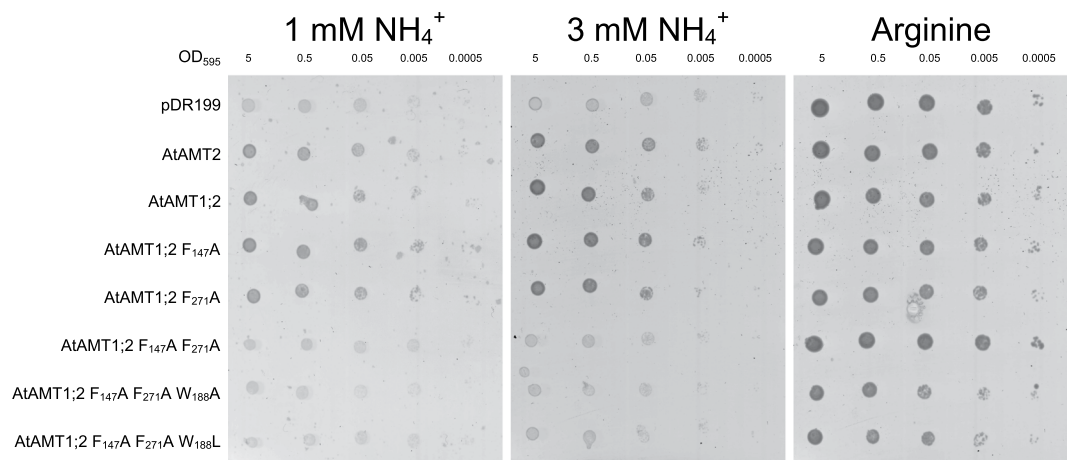


Figure 2. Single Phe mutants complement the growth of the $\Delta\Delta\Delta mep$ yeast on ammonium as the sole nitrogen source. $\Delta\Delta\Delta mep$ yeast was transformed with empty vector (pDR199) or pDR199 containing wildtype or mutant AtAMTs. The transformed yeast was spotted in 10-fold dilutions beginning with an $OD_{595} = 5$ on media containing arginine (control) or media containing ammonium (1 mM and 3 mM) as the sole nitrogen source. Yeast growth indicates ammonium transport. Four independent repetitions have been performed, the figure shows one representative experiment.

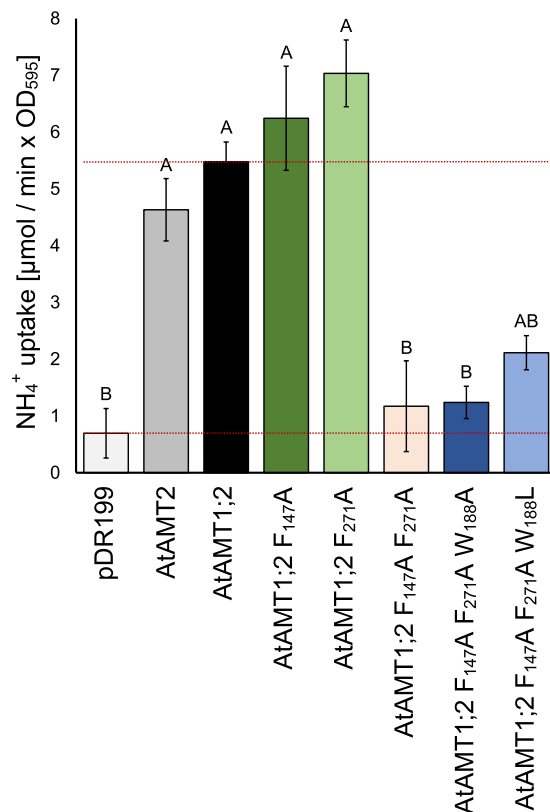


Figure 3. Single mutations in the Phe-gate do not affect the ammonium transport activity of AtAMT1;2. $\Delta\Delta\Delta mep$ yeast expressing the empty vector (pDR199), AtAMT2, AtAMT1;2 or the mutant versions of AtAMT1;2 was grown in liquid media, washed and re-suspended with an $OD_{595} = 5$ in media containing 3 mM NH_4^+ . The removal of ammonium from the medium was measured photometrically as described in the methods. The lower line in the graph indicates the background uptake by the empty vector control. The upper line indicates the transport rate of wild type AtAMT1;2. The experiment was performed in four repetitions. Data are shown as means with the error bars indicating the standard error. The data is showing the ammonium uptake by the yeast over time in $\mu\text{M} / \text{min} \times OD_{595}$. Significant differences with $p \leq 0.05$ are indicated by letters.

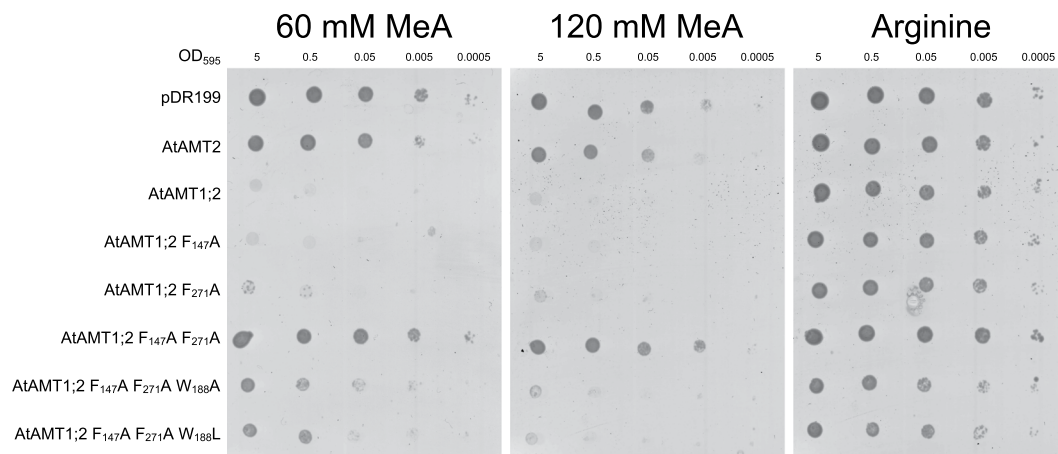


Figure 4. Methylammonium transport by AtAMT1;2 can be partially rescued by combining a W₁₈₈A/L mutation to the double Phe-gate mutant. $\Delta\Delta\Delta mep$ yeast was transformed with empty vector (pDR199) or pDR199 containing wildtype or mutant AtAMTs. The transformed yeast was spotted in 10-fold dilutions beginning with an OD₅₉₅ = 5 on media containing arginine as a nitrogen source and different concentrations of methylammonium (0 mM, 60 mM and 120 mM). Yeast growth indicates low or no methylammonium transport. Four independent repetitions have been performed, the figure shows one representative experiment.

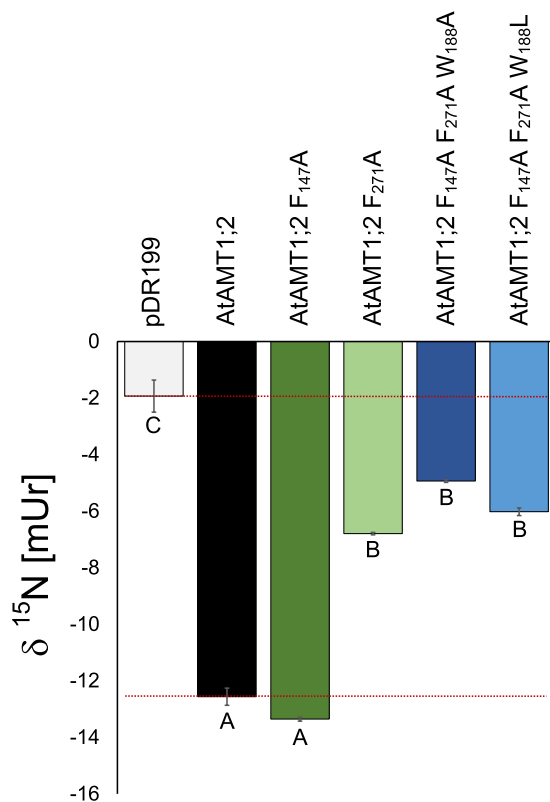


Figure 5. Increase in $\delta^{15}\text{N}$ values implies a partial loss of deprotonation in F₂₇₁A mutants. $\Delta\Delta\Delta mep$ yeast transfected with wildtype and mutant transporters were grown with 3 mM ammonium chloride in liquid culture and $\delta^{15}\text{N}$ values were assessed by isotope ratio mass spectrometry. The experiment was performed four times with two technical replications for mass spectrometry. Data are given as means \pm SD. Significant different values are indicated by different letters $p \leq 0.01$.

Discussion

The protein structures of several ammonium transporter proteins from various organisms indicate a conserved pore-occluding twin Phe-gate directly adjacent to the external ammonium recruitment site^{14–16,18,20–28}. Based on sequence identity and homology modeling^{5,9}, we propose a similar orientation of these two highly conserved

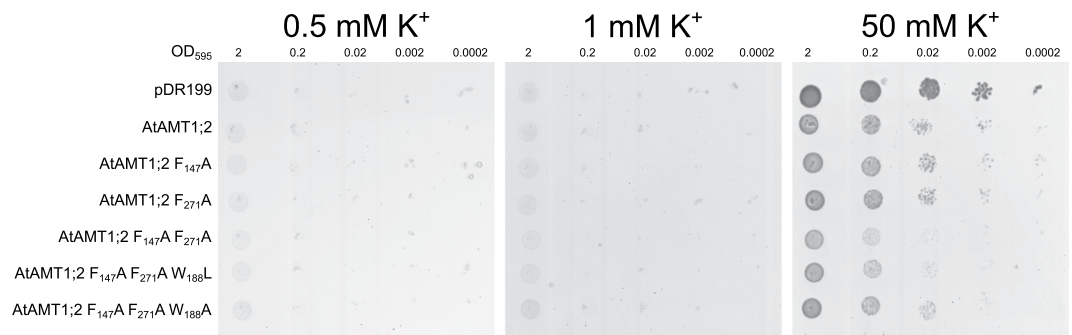


Figure 6. Growth complementation and functionality of AtAMT1;2 Phe-gate mutants in K^+ -uptake deficient $W\Delta 3$ yeast. Single, double and triple Phe-gate mutant plasmids were transformed into $W\Delta 3$ yeast. 10-fold dilutions of an $OD_{595} = 2$ culture were spotted on plates containing 0.5, 1 or 50 (control) mM potassium. The experiment was performed three times independently, representative data of one experiment are shown.

phenylalanines in plant AMT1 transporters as in AMT crystal structures. Members of the plant AMT1 family appear to transport net ammonium (as $NH_3 + H^+$)^{6,7}, whereas plant AMT2-like proteins seem to transport ammonia after NH_4^+ deprotonation^{8,9}. While the transport mechanism differs between individual AMT/Mep/Rh proteins (NH_3 , NH_4^+ or $NH_3 + H^+$ transport), the pore-lining residues and the basic mechanism with NH_4^+ deprotonation after NH_4^+ recruitment appear highly conserved^{9,10}. The external ammonium recruitment site including Asp₂₁₁, Ala₂₁₃ and Ser₂₇₅ (Fig. 1) and the function of the pore-occluding twin Phe-gate were addressed here. The D₂₁₁G and S₂₇₅G mutations strongly reduced or even impaired AMT activity, in line with a proposed role of substrate acquisition to the external recruitment site or for protein stability^{11–20}.

Knowing that the transport mechanism between EcAmtB and AtAMT1s may differ, the Phe-gate might vary in its importance for each individual transporters. In AtAMT1;2, exchange of individual phenylalanines to alanine yielded full transport function (Figs 2–4). For the first (outer) phenylalanine, this is in accordance with previous results in EcAmtB^{19,29}. The F₂₇₁A mutant in AtAMT1;2 was completely active while F₂₁₅ of EcAmtB was essential for ammonium and methylammonium transport^{19,29}. The double mutants F₁₄₇A F₂₇₁A in AtAMT1;2 and F₁₀₇A F₂₁₅A in EcAmtB were both inactive in ammonium and methylammonium transport. It is still interesting though, that in molecular dynamic simulations of this EcAmtB mutant (mimicking an open phenylalanine gate) the ammonium ion was still stabilized by the protein backbone in the position of the twin-His motif following the Phe-gate¹⁹. Notably, the introduction of the W₁₄₈L mutation in EcAmtB (W₁₈₈L in AtAMT1;2, respectively) partially rescued the transport function of the EcAmtB F₂₁₅L mutant and the F₁₀₇A F₂₁₅L double mutant, respectively. W₁₄₈ is located in the NH_4^+ recruitment site of the transporter and not directly part of the phenylalanine gate. It seems to play a minor role in stabilizing the ammonium charge in the recruitment pocket. The W₁₈₈L mutation will significantly increase the free space within this pocket, possibly facilitating the binding of the more bulky methylammonium¹⁴. This follows the observations from EcAmtB, in which the individual W₁₄₈L mutation strongly increased methylammonium transport²⁹. In AtAMT1;2 triple mutants (F₁₄₇A F₂₇₁A W₁₈₈A or F₁₄₇A F₂₇₁A W₁₈₈L) methylammonium transport was also restored (Fig. 4). Replacements in W₁₈₈, however, did not restore ammonium transport in the double mutant (Figs 2 and 3).

Isotope fractionation during ammonium transport into yeast cells had been proposed to result from easier deprotonation of the lighter N isotope substrate. Ultimately this would result in a higher abundance of the lighter isotope in total assimilated yeast N³². The isotope fractionation was reduced by the F₂₇₁ mutation, despite an unchanged transport rate, potentially indicating a partially lacking substrate deprotonation (Fig. 5). These results indicate an important role of F₂₇₁ in the deprotonation mechanism and thus selection against uncontrolled ion flux. Although the Phe-gate was suggested not to be directly involved in deprotonation¹⁹, F₂₇₁ might be important for stabilizing NH_4^+ or its charge during deprotonation. Deprotonation is then likely fulfilled by the adjacent twin-His motif. If slippage of NH_4^+ ions occurs, one may expect that ions of similar charge and size, such as K^+ are transported. However, none of the mutants or the wild type facilitated potassium uptake (Fig. 6). Instead, expression of all mutants impaired growth of the yeast on high K^+ , compared to the empty plasmid control, pointing to a general fitness decrease by AMTs in this yeast strain. Interestingly, the non-functional F₁₄₇A F₂₇₁A mutant was most inhibitory, showing that the transport function of the protein was not the cause of growth impairment.

Taken together, single mutations of the phenylalanines did not affect the transport activity of AtAMT1;2. Mutation of the inner Phe residue resulted in a partial loss of the AMT1;2 mediated isotope fractionation, indicating a partial loss of deprotonation. This as well indicates that the substrate is still protonated at the position of the phenylalanine gate, which would contradict a mechanism of ammonium deprotonation in the external vestibule^{15,16,18,20,26}. While deprotonation was partially lost in the mutants, all transporter versions were still selective against potassium.

In conclusion, not both Phe of the pore-occluding Phe-gate in the electrogenic AtAMT1;2 can simultaneously be replaced. While selective transport depends on substrate deprotonation³² (Fig. 7A), especially the inner Phe residue avoids NH_4^+ ion slippage through the pore. Mutation of F₂₇₁ may partially allow NH_4^+ ions to pass the pore without fractionation into H^+ and NH_3 (Fig. 7B). The loss of the aromatic structure in the F₂₇₁A mutant might decrease the NH_4^+ coordination in this position and thereby reduce the deprotonation dependence. Mutation of W₁₈₈ provides a pore recruitment constitution that improves methylammonium entrance to the pore. Therefore, W₁₈₈ recruits NH_4^+ , but prevents methylammonium entry into the AMT pore.

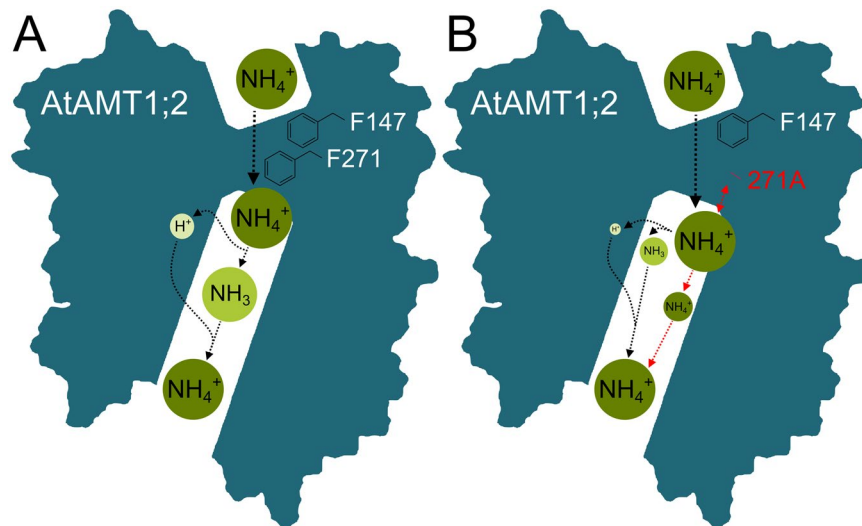


Figure 7. Schematic model of the transport mechanism in the AtAMT1;2 wildtype and the $F_{271}A$ mutant. (A) In the wildtype transporter, NH_4^+ passes the pore and is deprotonated after crossing about 40% of the membrane electric field. On the cytoplasmic side, it is re-protonated to NH_4^+ by a co-transported proton. (B) In the $F_{271}A$ mutant, the transport – deprotonation coupling is partially lost. NH_4^+ might directly slip through the AMT pore (red arrows). The red bidirectional arrow indicates reduced coordination of the ammonium ion. This possible loss of ion stabilization might reduce deprotonation efficiency. The schematic model is based on a homology model of AtAMT1;2⁷. The structural fitting for the homology model was done using the crystal structures of AfAMT-1³⁸ and EcAmB^{11,12}.

Material and Methods

Plasmid constructs. Briefly, the open reading frames of AtAMT1;2 (At1g64780), AtAMT2 (At2g38290) and NeRh1 (gi_30248465) were amplified from genomic DNA or cDNA of *Arabidopsis thaliana* Col-0 wildtype and cDNA of *Nitrosomonas europaea* respectively. Using specific restriction enzymes they were then subcloned into the yeast expression vector pDR199^{7,9,31}. The mutant constructs were based on this original construct. To introduce the mutations, forward and reverse mismatch primers were designed and mutant constructs were produced by mutagenesis PCR using S7 Fusion High-Fidelity DNA Polymerase (Biozym Scientific, Hessisch Oldendorf, Germany). Template DNA was digested by DpnI. To verify the mutations and exclude other mutations the constructs were Sanger sequenced (Eurofins Genomics, Ebersberg, Germany).

Yeast transformation. The plasmids containing the respective open reading frames were heat shock-transformed in the ura^- ammonium transporter defective yeast strain (31019b; $\Delta\Delta\Delta\text{mep}$)³³ and the potassium transporter defective *Saccharomyces cerevisiae* strain W Δ 3 (MATa, *ade2*, *ura3*, *trp1*, *trk1* Δ ::LEU2, *trk2* Δ ::HIS3)³⁴. Selection for transformed yeast was done on solid arginine media (20 g \times l⁻¹ Agar, 1.7 g \times l⁻¹ YNB w/o amino acids and ammonium sulfate (Difco), supplemented with 20 g \times l⁻¹ glucose and 1 g \times l⁻¹ arginine (Arg) as nitrogen source) or on Arg phosphate minimal media³⁵ containing 100 mM K⁺.

Yeast growth assays. Yeast was grown in liquid Arg medium until OD₅₉₅ (optical density at 595 nm) reached 0.6–0.8. Cells were harvested, washed three times and resuspended in water to a final OD₅₉₅ of 2 or 5. 10 μ l of these cells and 10-fold dilutions were spotted on Arg medium with or without MeA (60 mM or 120 mM), or media containing no Arg, but 1 mM or 3 mM NH_4Cl as sole nitrogen source. For growth on selective potassium media, yeast was spotted as 10 fold dilutions of OD₅₉₅ of 2, on Arg phosphate minimal media containing different concentrations of K⁺. Pictures were taken after 3 to 5 days of growth, the experiments were performed in three or four independent repetitions.

Ammonium uptake assay. To determine ammonium uptake rates of the $\Delta\Delta\Delta\text{mep}$ yeast expressing the different ammonium transporter constructs, an ammonium uptake assay was conducted. Cells were grown overnight in 50 ml Arg medium supplemented with 1 g \times l⁻¹ arginine at 28 °C, washed three times in water, and resuspended in Arg medium with 3 mM ammonium chloride at OD₅₉₅ of 3. The cultures were incubated with shaking (200 rpm) at 28 °C in a 30 ml volume and 500 μ l samples were taken every 30 min until 3 h. The cells were pelleted and 300 μ l supernatant was separated from the pellet and stored at 4 °C. 40 μ l of the supernatant was added to 760 μ l OPA (o-phthaldialdehyde) solution (540 mg o-phthaldialdehyde, 10 ml ethanol, 50 μ l β -mercaptoethanol, 0.2 M phosphate buffer, pH 7.3 ad 100 ml) to quantify the remaining ammonium³⁶. After 20 min of incubation in the dark, the extinction at 420 nm was measured. As a reference, 760 μ l OPA plus 40 μ l water was used. The system was calibrated with ammonium chloride concentrations from 0 to 5 mM. The experiment was performed in four independent repetitions.

Change in the natural $\delta^{15}\text{N}$. Discrimination of the transporters against the heavy ^{15}N isotope was determined in yeast. $\Delta\Delta\Delta_{mep}$ yeast was transformed as described above. Cells were grown overnight in 50 ml SD medium with $1\text{ g} \times \text{l}^{-1}$ arginine at 28°C . OD_{595} of the overnight culture was determined and a new 150 ml culture in SD medium with 3 mM NH_4^+ as sole nitrogen source was inoculated with OD_{595} 0.01. Cultures were incubated at 28°C with shaking at 120 rpm. Cultures were harvested when OD_{595} reached approx. 0.3. Cells were washed two times, pelleted, freeze-dried and $\delta^{15}\text{N}$ ratios were determined by isotope ratio mass spectrometry. For IRMS analysis approx. 0.5 mg of yeast or standard material was balanced into tin cups (HEKAtech, Wegberg, Germany). Standard material used was USGS41, L-glutamic acid with $\delta^{15} = 47.6\text{‰}$ air N_2 . For measurement an element analyzer (EuroVector, HEKAtech, Wegberg, Germany) coupled to a mass spectrometer (Delta plus Advantage, Thermo Scientific, Bremen, Germany) was used. δ^{15} values are calculated vs. Air- N_2 using the following equation: $\delta\text{‰} = (\text{Isotope ratio of sample}/\text{Isotope ratio of air} - 1) \times 1000$. Data are given as means from two independent experiments with two biological replicates each \pm SD. Significance was calculated by one-way ANOVA followed by a Tukey HSD test.

Data availability

All data are part of the manuscript.

Received: 19 June 2019; Accepted: 31 October 2019;

Published online: 14 November 2019

References

- Smith, F. A. & Walker, N. A. Entry of methylammonium and ammonium ions into Chara internodal cells. *J. Exp. Bot.* **29**, 107–120 (1978).
- Pelley, J. L. & Bannister, T. T. Methylamine uptake in the green alga *Chlorella pyrenoidosa*. *J. Phycol.* **15**, 110–112 (2008).
- Kleiner, D. The transport of NH_3 and NH_4^+ across biological membranes. *Biochim. Biophys. Acta - Rev. Bioenerg.* **639**, 41–52 (1981).
- Boussiba, S., Resch, C. M. & Gibson, J. Ammonia uptake and retention in some cyanobacteria. *Arch. Microbiol.* **138**, 287–292 (1984).
- Ludewig, U. *et al.* Molecular mechanisms of ammonium transport and accumulation in plants. *FEBS Lett.* **581**, 2301–2308 (2007).
- Mayer, M., Dynowski, M. & Ludewig, U. Ammonium ion transport by the AMT/Rh homologue LeAMT1;1. *Biochem. J.* **396**, 431–7 (2006).
- Neuhäuser, B., Dynowski, M., Mayer, M. & Ludewig, U. Regulation of NH_4^+ transport by essential cross talk between AMT monomers through the carboxyl tails. *Plant Physiol.* **143**, 1651–9 (2007).
- Guether, M. *et al.* A Mycorrhizal-Specific Ammonium Transporter from *Lotus japonicus* Acquires Nitrogen Released by Arbuscular Mycorrhizal Fungi. *Plant Physiol.* **150**, 73–83 (2009).
- Neuhäuser, B., Dynowski, M. & Ludewig, U. Channel-like NH_3 flux by ammonium transporter AtAMT2. *FEBS Lett.* **583**, 2833–8 (2009).
- Neuhäuser, B., Dynowski, M. & Ludewig, U. Switching substrate specificity of AMT/MEP/Rh proteins. *Channels* **8**, 496–502 (2014).
- Khademi, S. *et al.* Mechanism of ammonia transport by Amt/MEP/Rh: structure of AmtB at 1.35 Å. *Science* **305**, 1587–94 (2004).
- Zheng, L. *et al.* The mechanism of ammonia transport based on the crystal structure of AmtB of *Escherichia coli*. *Proc. Natl. Acad. Sci. USA* **101**, 17090–5 (2004).
- Lupo, D. *et al.* The 1.3-Å resolution structure of *Nitrosomonas europaea* Rh50 and mechanistic implications for NH_3 transport by Rhesus family proteins. *Proc. Natl. Acad. Sci.* **104**, 19303–19308 (2007).
- Nygaard, T. P., Alfonso-Prieto, M., Peters, G. H., Jensen, M. Ø. & Rovira, C. Substrate Recognition in the *Escherichia coli* Ammonia Channel AmtB: A QM/MM Investigation. *J. Phys. Chem. B* **114**, 11859–11865 (2010).
- Nygaard, T. P., Rovira, C., Peters, G. H. & Jensen, M. Ø. Ammonium recruitment and ammonia transport by *E. coli* ammonia channel AmtB. *Biophys. J.* **91**, 4401–12 (2006).
- Ishikita, H. & Knapp, E.-W. Protonation States of Ammonia/Ammonium in the Hydrophobic Pore of Ammonia Transporter Protein AmtB. *J. Am. Chem. Soc.* **129**, 1210–1215 (2007).
- Luzhkov, V. B., Almlöf, M., Nervall, M. & Aqvist, J. Computational study of the binding affinity and selectivity of the bacterial ammonium transporter AmtB. *Biochemistry* **45**, 10807–14 (2006).
- Bostick, D. L. & Brooks, C. L. Deprotonation by dehydration: The origin of ammonium sensing in the AmtB channel. *PLoS Comput. Biol.* **3**, e22 (2007).
- Javelle, A. *et al.* Substrate binding, deprotonation, and selectivity at the periplasmic entrance of the *Escherichia coli* ammonia channel AmtB. *Proc. Natl. Acad. Sci. USA* **105**, 5040–5 (2008).
- Lin, Y., Cao, Z. & Mo, Y. Molecular dynamics simulations on the *Escherichia coli* ammonia channel protein AmtB: mechanism of ammonia/ammonium transport. *J. Am. Chem. Soc.* **128**, 10876–84 (2006).
- Lamoureux, G., Klein, M. L. & Bernèche, S. A stable water chain in the hydrophobic pore of the AmtB ammonium transporter. *Biophys. J.* **92**, L82–4 (2007).
- Akgun, U. & Khademi, S. Periplasmic vestibule plays an important role for solute recruitment, selectivity, and gating in the Rh/Amt/MEP superfamily. *Proc. Natl. Acad. Sci. USA* **108**, 3970–5 (2011).
- Wang, J. *et al.* Molecular dynamics simulations on the mechanism of transporting methylamine and ammonia by ammonium transporter AmtB. *J. Phys. Chem. B* **114**, 15172–9 (2010).
- Lin, Y., Cao, Z. & Mo, Y. Functional role of Asp160 and the deprotonation mechanism of ammonium in the *Escherichia coli* ammonia channel protein AmtB. *J. Phys. Chem. B* **113**, 4922–9 (2009).
- Yang, H., Xu, Y., Zhu, W., Chen, K. & Jiang, H. Detailed mechanism for AmtB conducting $\text{NH}_4^+/\text{NH}_3$: Molecular dynamics simulations. *Biophys. J.* **92**, 877–85 (2007).
- Cao, Z., Mo, Y. & Thiel, W. Deprotonation mechanism of NH_4^+ in the *Escherichia coli* ammonium transporter AmtB: insight from QM and QM/MM calculations. *Angew. Chem. Int. Ed. Engl.* **46**, 6811–5 (2007).
- Bostick, D. L. & Brooks, C. L. On the equivalence point for ammonium (de)protonation during its transport through the AmtB channel. *Biophys. J.* **92**, L103–5 (2007).
- Liu, Y. & Hu, X. Molecular determinants for binding of ammonium ion in the ammonia transporter AmtB - A quantum chemical analysis. *J. Phys. Chem. A* **110**, 1375–81 (2006).
- Hall, J. A. & Kustu, S. The pivotal twin histidines and aromatic triad of the *Escherichia coli* ammonium channel AmtB can be replaced. *Proc. Natl. Acad. Sci. USA* **108**, 13270–4 (2011).
- Zidi-Yahiaoui, N. *et al.* Functional analysis of human RhCG: comparison with *E. coli* ammonium transporter reveals similarities in the pore and differences in the vestibule. *Am. J. Physiol. Physiol.* **297**, C537–C547 (2009).
- Weidinger, K. *et al.* Functional and physiological evidence for a rhesus-type ammonia transporter in *Nitrosomonas europaea*. *FEMS Microbiol. Lett.* **273**, 260–7 (2007).

32. Ariz, I. *et al.* Nitrogen isotope signature evidences ammonium deprotonation as a common transport mechanism for the AMT-Mep-Rh protein superfamily. *Sci. Adv.* **4**, eaar3599 (2018).
33. Marini, A. M., Soussi-Boudekou, S., Vissers, S. & Andre, B. A family of ammonium transporters in *Saccharomyces cerevisiae*. *Mol. Cell. Biol.* **17**, 4282–4293 (1997).
34. Haro, R., Sainz, L., Rubio, F. & Rodriguez-Navarro, A. Cloning of two genes encoding potassium transporters in *Neurospora crassa* and expression of the corresponding cDNAs in *Saccharomyces cerevisiae*. *Mol. Microbiol.* **31**, 511–520 (1999).
35. Rodriguez-Navarro, A. & Ramos, J. Dual system for potassium transport in *Saccharomyces cerevisiae*. *J. Bacteriol.* **159**, 940–5 (1984).
36. Benson, J. R. & Hare, P. E. O-phthalaldehyde: fluorogenic detection of primary amines in the picomole range. Comparison with fluorescamine and ninhydrin. *Proc. Natl. Acad. Sci.* **72**, 619–622 (1975).
37. van den Berg, B. *et al.* Structural basis for Mep2 ammonium transporter activation by phosphorylation. *Nat. Commun.* **7**, 11337 (2016).
38. Andrade, S. L. A., Dickmanns, A., Ficner, R. & Einsle, O. Crystal structure of the archaeal ammonium transporter Amt-1 from *Archaeoglobus fulgidus*. *Proc. Natl. Acad. Sci. USA* **102**, 14994–9 (2005).

Acknowledgements

We thank D. Schnell for technical assistance and help with the yeast uptake experiments. Further we thank W. Armbruster for help with the ¹⁵N measurements. We thank F. Rubio for supplying the WΔ3 yeast strain.

Author contributions

R.M. and B.N. performed cloning and the initial ammonium yeast experiments. P.G., T.I. and R.P. repeated experiments. P.G. performed isotope fractionation experiments and potassium growth. U.L. and B.N. planned the experiments. P.G. and B.N. wrote the manuscript. P.G., R.M., T.I., R.P., U.L. and B.N. revised the manuscript. B.N. is the corresponding author.

Competing interests

The authors declare no competing interests.

Additional information

Supplementary information is available for this paper at <https://doi.org/10.1038/s41598-019-53333-9>.

Correspondence and requests for materials should be addressed to B.N.

Reprints and permissions information is available at www.nature.com/reprints.

Publisher's note Springer Nature remains neutral with regard to jurisdictional claims in published maps and institutional affiliations.



Open Access This article is licensed under a Creative Commons Attribution 4.0 International License, which permits use, sharing, adaptation, distribution and reproduction in any medium or format, as long as you give appropriate credit to the original author(s) and the source, provide a link to the Creative Commons license, and indicate if changes were made. The images or other third party material in this article are included in the article's Creative Commons license, unless indicated otherwise in a credit line to the material. If material is not included in the article's Creative Commons license and your intended use is not permitted by statutory regulation or exceeds the permitted use, you will need to obtain permission directly from the copyright holder. To view a copy of this license, visit <http://creativecommons.org/licenses/by/4.0/>.

© The Author(s) 2019